NOVEM 10-12 JANUARY • AUCKLAND • NEW ZEALAND 2023

LOCALLY RESONANT METAMATERIALS WITH MULTIMODAL RESONATORS FOR SOUND INSULATION IMPROVEMENT

Daniele Giannini[1*], Mattias Schevenels[2] and Edwin P.B. Reynders[1]

[1]KU Leuven, Department of Civil Engineering, Structural Mechanics Section, Kasteelpark Arenberg 40, 3001, Leuven, Belgium
[*]Email: daniele.giannini@kuleuven.be

[2] KU Leuven, Department of Architecture, Architectural Engineering Research Group, Kasteelpark Arenberg 1, 3001, Leuven, Belgium

ABSTRACT

Locally resonant metamaterials are used to increase the sound insulation of a host structure, by introducing bandgaps for wave propagation. While most solutions employ periodic layouts with translational resonators, this work investigates the potential of rotational and multimodal resonators. A comprehensive analytical model of sound insulation, based on dynamic effective mass density, is first presented. It is then demonstrated how multimodal locally resonant metamaterials can suppress the broad coincidence dip in the diffuse transmission loss of orthotropic host plates, and the geometry of two realizable multimodal resonators is optimized to maximize broadband sound insulation.

1 INTRODUCTION

An emerging research field is related to locally resonant metamaterials (LRMs) [1], that allow to achieve resonance-based wave propagation bandgaps by local resonators periodically attached to a host structure. LRMs can be applied to obtain acoustic partitions with improved sound transmission loss (TL), e.g. single LRM panels with suppressed TL coincidence dip.

While most literature works focus on LRM panels with translational resonators, in this work we investigate the potential of rotational and multimodal resonators. In order to predict the impact on sound insulation performance, we first present a comprehensive analytical description based on dynamic effective mass density (Section 2). We then show how multimodal LRMs can be effective in broadband sound insulation improvements, by applying LRMs to suppress the broad coincidence TL dip of orthotropic plates and optimizing two selected resonator layouts (Section 3). Finally, we give conclusions and remarks (Section 4).

2 ORTHOTROPIC LRM PLATES WITH MULTIMODAL RESONATORS

2.1 Sound TL of bare orthotropic plates

For a plane incident sound wave with propagation direction defined by angles (ϕ, θ) (Figure 1), a bending wave in the plate is induced with trace wavenumber $k = \frac{\omega}{c}\sin\theta$, and projections along the x and y directions $k_\mathrm{x} = \frac{\omega}{c}\sin\theta\cos\phi$ and $k_\mathrm{y} = \frac{\omega}{c}\sin\theta\sin\phi$. The sound TL of orthotropic plates for diffuse incident field can be analytically computed by integrating the transmission coefficients for single incident direction $\tau(\phi, \theta)$ [2]:

$$R = -10\log_{10}\tau_\mathrm{d} \qquad \tau_\mathrm{d} = \frac{\int_0^{2\pi}\int_0^{\pi/2}\tau(\phi,\theta)\sin\theta\cos\theta\mathrm{d}\theta\mathrm{d}\phi}{\int_0^{2\pi}\int_0^{\pi/2}\sin\theta\cos\theta\mathrm{d}\theta\mathrm{d}\phi}$$
$$\tau(\phi,\theta) = \left|\frac{2\rho_0 c(1-\sin^2\theta)^{-1/2}}{2\rho_0 c(1-\sin^2\theta)^{-1/2} - (\mathrm{j}/\omega)(D(\phi)k^4 - \rho h\omega^2)}\right|^2 \tag{1}$$

where h and ρ are the thickness and the mass density of the plate, ρ_0 and c are the mass density and the speed of sound in the surrounding fluid. $D(\phi) = D_\mathrm{x}\cos^4\phi + 2H\cos^2\phi\sin^2\phi + D_\mathrm{y}\sin^4\phi$ is the bending stiffness of the plate in the direction ϕ, which depends on the bending stiffnesses D_x and D_y along the x and y directions, and on the torsional stiffness H.

At the critical frequency $f_\mathrm{c}(\phi) = \frac{c^2}{2\pi}\sqrt{\frac{\rho h}{D(\phi)}}$ the speed of the bending waves equals the speed of sound in air, and a sharp TL dip appears. In orthotropic plates, f_c depends on the propagation direction ϕ, and for diffuse incident fields the coincidence TL dip covers a broader band.

2.2 Sound TL of orthotropic LRM plates with SDOF resonators

Let's consider orthotropic LRM plates with single degree of freedom (SDOF) vertical resonators (Figure 1a) and SDOF rotational resonators (Figure 1b). The translational and rotational inertia of the resonators are indicated as m_z and J_ry, the related stiffnesses as k_z and k_ry. If the size of the unit cell (UC) is $L_\mathrm{x} \times L_\mathrm{y}$, and $n = 1/(L_\mathrm{x}L_\mathrm{y})$, the dynamic effective mass densities of LRM plates with SDOF translational and rotational resonators are:

$$\rho_\mathrm{eff,z} = \rho + \frac{nk_\mathrm{z}m_\mathrm{z}}{h\left(k_\mathrm{z} - m_\mathrm{z}\omega^2\right)}, \quad \rho_\mathrm{eff,ry} = \rho + \frac{nk_\mathrm{x}^2 k_\mathrm{ry}J_\mathrm{ry}}{h\left(k_\mathrm{ry} - J_\mathrm{ry}\omega^2\right)}, \quad \rho_\mathrm{eff,rx} = \rho + \frac{nk_\mathrm{y}^2 k_\mathrm{rx}J_\mathrm{rx}}{h\left(k_\mathrm{rx} - J_\mathrm{rx}\omega^2\right)} \tag{2}$$

The effective mass densities in Eq. (2) can be used in place of the static mass density of the plate ρ in Eq. (1) to study the TL of LRM panels. In particular, a bandgap is expected close to the fixed-base resonance frequencies of the resonators, along with an associated TL peak.

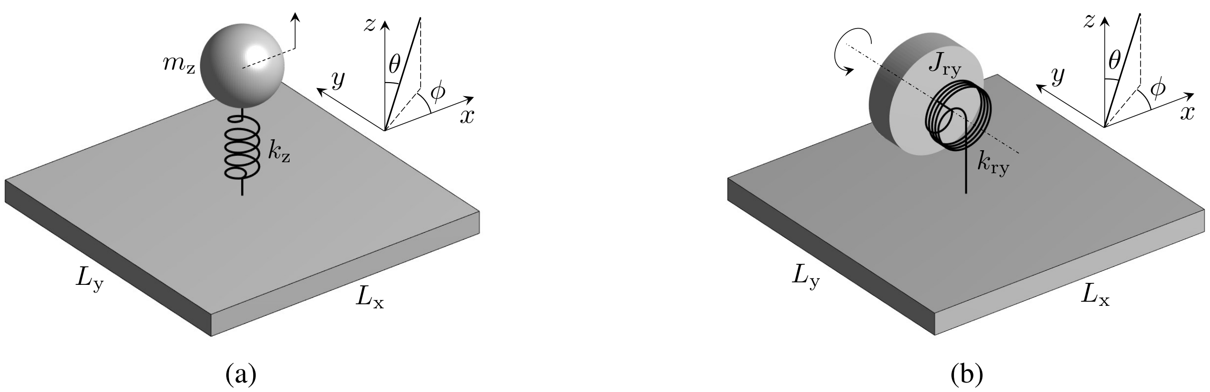

Figure 1: Scheme of the LRM plate UC when attaching (a) translational and (b) rotational resonators, along with the angles (ϕ, θ) defining the direction of incident plane waves.

2.3 Sound TL of orthotropic LRM plates with multimodal resonators

For complex resonators with multiple modes, each mode can be associated with translational and rotational inertial contributions. These are found by discretizing the resonator layout by finite elements, computing its first n_m fixed-base modes, and finding the related modal effective masses $m_{i,k}^\mathrm{eff}$ of each mode k along the kinematic direction $i = z, \theta_\mathrm{x}, \theta_\mathrm{y}$ [3]. The modal effective masses are included in the effective mass density of the LRM plate as:

$$\rho_\mathrm{eff} = \rho\alpha_\mathrm{static} + \sum_{k=1}^{n_\mathrm{m}} \frac{n}{h}\left(\frac{k_{\mathrm{z},k}^\mathrm{eff} m_{\mathrm{z},k}^\mathrm{eff}}{k_{\mathrm{z},k}^\mathrm{eff} - m_{\mathrm{z},k}^\mathrm{eff}\omega^2} + \frac{k_\mathrm{y}^2 k_{\theta_\mathrm{x},k}^\mathrm{eff} m_{\theta_\mathrm{x},k}^\mathrm{eff}}{k_{\theta_\mathrm{x},k}^\mathrm{eff} - m_{\theta_\mathrm{x},k}^\mathrm{eff}\omega^2} + \frac{k_\mathrm{x}^2 k_{\theta_\mathrm{y},k}^\mathrm{eff} m_{\theta_\mathrm{y},k}^\mathrm{eff}}{k_{\theta_\mathrm{y},k}^\mathrm{eff} - m_{\theta_\mathrm{y},k}^\mathrm{eff}\omega^2}\right) \tag{3}$$

where $\alpha_\mathrm{static} = 1 + m_\mathrm{ratio} - \sum_{k=1}^{n_\mathrm{m}} \frac{m_{\mathrm{z},k}^\mathrm{eff}}{m_\mathrm{UC}}$ includes the quasi-static contributions of higher order modes, and $k_{i,k}^\mathrm{eff} = m_{i,k}^\mathrm{eff}\omega_{\mathrm{r},k}^2$ are the modal effective stiffnesses. m_ratio is the ratio between the resonator mass and the mass of the host structure $m_\mathrm{UC} = \rho h L_\mathrm{x} L_\mathrm{y}$ within the UC.

3 OPTIMIZATION OF MULTIMODAL RESONATOR LAYOUTS

The efficient analytical TL predictions for LRM plates can be combined with numerical optimization, in order to optimize the geometry of realizable multimodal resonators when maximizing broadband sound insulation. Here we consider an orthotropic plate (h = 15 mm, ρ = 1200 kg/m^3, D_x = 1500 Nm, D_y = 4500 Nm, H = 2598 Nm, η_0 = 0.05) surrounded by air (c = 341 m/s, ρ_0 = 1.21 kg/m^3), and the two resonator layouts in Figures 2a and 2b, made of polymethyl methacrylate (PMMA, E = 4850 MPa, ν = 0.31, ρ = 1200 kg/m^3, η = 0.05), are optimized through the reported design variables. Layout 1 consists of a mass suspended by a vertical beam, and the two main modes of interest are related to rotations of the mass around the x and y axes. Layout 2 consists of a translational resonator with two resonating units, composed by cantilever beams with attached end-point masses, and the two main modes of interest are related to the vertical motion of the masses.

The resonator layouts are optimized by maximizing the single number rating R_A for broadband sound insulation [4], while keeping the resonator mass lower than 20% of the host plate mass. The optimization problem is solved using a Genetic Algorithm (GA), and the optimized resonator layouts are shown in Figures 2a and 2b. The TL curves of the resulting LRM plates are shown in Figures 2c and 2d, along with a comparison with bare plates respectively with the original mass and with the same mass as the LRM plates. We see how each mode of interest introduces a TL peak. For Layout 1, the modes of interest are the two rotational ones around x and y. For Layout 2 the main peaks are related to the two translational modes (modes 3 and 4), but also smaller peaks related to rotational modes around x (modes 1 and 2) are exploited by the optimizer. For both layouts, the coincidence TL dip of the original bare plate is suppressed by the introduced resonant TL peaks: this leads to an improvement of R_A by around 4 dB with respect to bare plates with equivalent mass.

4 CONCLUSIONS

In this work, orthotropic locally resonant metamaterial (LRM) plates with rotational and multimodal resonators have been studied. An efficient analytical description of the sound transmission loss, based on dynamic effective mass density, has been proposed and combined with numerical optimization to automatically design the geometrical layout of two multimodal resonators. The layouts have been optimized to maximize broadband sound insulation through the single number rating R_A, achieving significant broadband TL improvements and suppressing the broad coincidence dip of the original bare orthotropic plate.

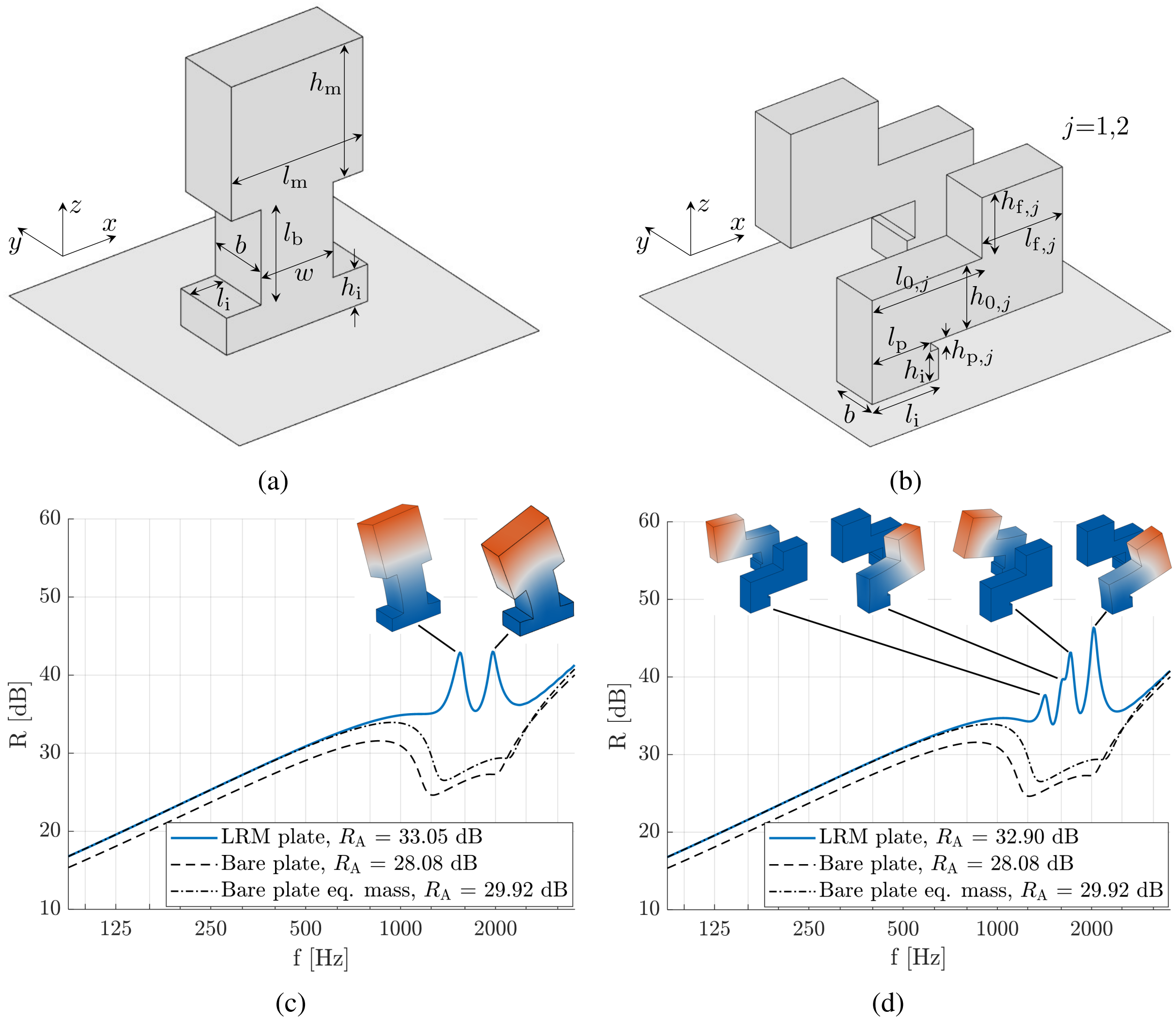

Figure 2: Optimized orthotropic LRM plates with multimodal resonators and associated TL curves: (a,c) Layout 1, (b,d) Layout 2.

ACKNOWLEDGEMENTS

The presented work has been carried out within the ERC Starting Grant 714591 VirBAcous. The authors gratefully acknowledge the financial support of the European Research Council.

REFERENCES

[1] C. Claeys, K. Vergote, P. Sas, and W. Desmet. On the potential of tuned resonators to obtain low-frequency vibrational stop bands in periodic panels. *Journal of Sound and Vibration*, 332(6):1418–1436, 2013.

[2] F. Fahy and P. Gardonio. *Sound and structural vibration: radiation, transmission and response*. Academic Press, Oxford, UK, 2nd edition, 2007.

[3] J.J. Wijker. *Modal Effective Mass*, pages 247–263. Springer Berlin Heidelberg, 2008.

[4] International Organization for Standardization. *ISO 717-1: Acoustics – Rating of sound insulation in buildings and of building elements – Part 1: Airborne sound insulation*, 2013.